Available online at www.sciencedirect.com
ScienceDirect
Trans. Nonferrous Met. Soc. China 22(2012) s138−s142
Transactions of Nonferrous Metals Society of China
www.tnmsc.cn

Fabrication and characteristics of strontium barium niobate/ barium strontium titanate ceramics by powder−sol method

SHAN Lian-wei, WANG Feng-chun, WANG Ji-hua, WU Ze, HAN Zhi-dong, DONG Li-min, ZHANG Xian-you
Department of Materials Science and Engineering, Harbin University of Science and Technology, Harbin 150040, China

Received 9 July 2012; accepted 14 August 2012

Abstract: Barium strontium titanate ($Ba_{1-x}Sr_xTiO_3$, BST) and strontium barium niobate ($Sr_xBa_{1-x}Nb_2O_6$, SBN) are important ferroelectric materials with excellent pyroelectric, dielectric properties and faster response time of infrared radiation. SBN/BST composite ceramics with different mole ratios of Nb and Ti were fabricated using a powder-sol (P-S) method with Nb_2O_5 fine powders suspended in the barium strontium titanate (BST in short) sol solution. The X-ray diffraction results indicate that three intermediate phases, i.e. TiO_2, $BaNb_2O_6$ and $SrNb_2O_6$, are developed during the formation of SBN-BST. Powders obtained from dried gels are calcined at 800 ℃ for 3 h. The Ti_{2p} spectra of only one spin-orbit doublet are observed, which indicates one 4+ chemical state in the composite ceramics. The binding energies of Nb element depend strongly on composition.
Key words: barium strontium titanate; strontium barium niobate; binding energy

1 Introduction

Barium strontium titanate ($Ba_{1-x}Sr_xTiO_3$, BST) and strontium barium niobate ($Sr_xBa_{1-x}Nb_2O_6$, SBN) have been widely studied due to their outstanding properties and potential applications. They are important ferroelectric materials with excellent pyroelectric, dielectric properties and faster response time of infrared radiation [1−3]. Because of the above important technological applications, the preparation methods, microstructure, properties and doping on SBN, BST ceramics have been widely reported [4−6]. By ordinary ceramic sintering technique, SBN-BST composite ceramics have been fabricated [7,8]. However, the results show that uniformity of microstructure is not easily controlled, and the higher sintering temperature is required than sol-gel technique. It is easy to make BST by sol-gel through titanic alkoxide using titanium hydroxide as raw materials [9]. Nb_2O_5 is as a raw material to make some $Sr_xBa_{1-x}Nb_2O_6$ in the composite ceramics. The formation center of $Sr_xBa_{1-x}Nb_2O_6$ consists of a Nb_2O_5 core. However, the preparation and characterization on SBN-BST composite ceramics by powder-sol (P-S) has not yet been reported, and little is known about the formation and microstructure of SBN-BST composite ceramics. So, there has been a great interest in the preparation of $y(Ba_{0.7}, Sr_{0.3})Nb_2O_6(1-y)(Ba_{0.7}, Sr_{0.3})TiO_3$ (SBN-BST) composite ceramics as well as in the microstructure.

The use of P-S processing can not only form homogeneous structure, but also decrease the sintering temperature. In the present work, the fabrication of SBN-BST ceramics produced from P-S method was reported and the effects of different mole ratios of Nb and Ti on the composite materials were studied.

2 Experimental

$Ba(C_2H_3O_2)_2$ (99.5%), $Sr(C_2H_3O_2)_2{\cdot}1/2H_2O$ (99.5%), Nb_2O_5 (99.9%) and La_2O_3 (99.9%) were used as starting materials. According to the compositions of $y(Ba_{0.7}, Sr_{0.3})Nb_2O_6(1-y)(Ba_{0.7}, Sr_{0.3})TiO_3$, they were weighed. The y values in SBN-BST were 0, 0.1, 0.2, 0.3, 0.4, 0.5, 0.6, 0.7, respectively. The A solution was prepared with barium acetate [$Ba(C_2H_3O_2)_2$] and strontium acetate [$Sr(C_2H_3O_2)_2{\cdot}1/2H_2O$] as the precursor, acetic acid and deionized water as the main solvents, and deionized water also as the accelerating agent. Tetrabutyl titanate [$Ti(OBu)_4$] is unstable due to its high sensitivity to the

Foundation item: Project (2008RFQXG070) supported by the Science and Technology Innovation Special Foundation of Harbin City, China; Project (F200927) supported by Natural Science Foundation of Heilongjiang Province, China
Corresponding author: SHAN Lian-wei; Tel: +86-13030069275; E-mail: Shlw0531@163.com

moisture in air. Here, anhydrous alcohol B solution was used. Nb_2O_5 fine powder was suspended in B solution with the magnetic stirring and then ultrasonic was used to make the powder disperse uniformly in the B solution. The precursor A solution was mixed with B solution under magnetic stirring and ultrasonic stirring. Gelation started after B solution was added into A solution. In order to control the viscosity of the sol, the velocity of B solution adding into A solution has to be controlled. The solid xerogel was obtained after about 0.5 h. The xerogel was calcined in air at different temperatures to analyze the formation course of composite ceramics. The xerogel was calcined at 800 °C for 3 h to burn off organics and partly crystallize the material, and then crushed and ball milled for 8 h. After drying, the fine powder was compressed into disks of 13 mm in diameter and 2 mm in thickness under 300 MPa. The disks were sintered at different temperatures for 3 h to analyze the phase structure of composite ceramics. Finally, the pre-sintered disks were sintered at 1200 °C for 3 h to produce dense ceramics.

The crystallization behavior of the ceramics were analyzed by X-ray diffraction (XRD, Model D/MAX-3B, Tokyo, Japan) excited with Cu K_α radiation, a sampling interval of 0.02°, and a scan speed of 4 (°)/min. The fracture surface morphology was studied by scanning electron microscope (SEM, FEISirion 200, Netherlands). The surface XPS analysis was performed with a Perkin Elmer PHI5300 ESCA/610 SAM using a spherical capacitance analyzer, and all spectra were referenced to the adventitious C_{1s} peak at 284.6 eV. Mg K_α(1253.6 eV) radiation was adopted as the excitation source, operating at 250 W, 125 kV and 20 mA. The operating pressure of instrument chamber was in the order of 10^{-9} Pa. The measured spectra were decomposed into Gaussian components (20%) and Lorentzian components (80%) with symmetry by least squares fitting method after subtracting Shirley background.

3 Results and discussion

Dried gel powders with Nb^{5+} content of y=0.5 were heat-treated at various temperatures to obtain the perovskite phase and tetragonal tungsten bronze phase. Fig. 1 shows the X-ray diffraction patterns of composite powders. It illustrates the evolution of crystallization of the BSTN powders with increasing the calcining temperature [7]. After calcined at 700 °C for 3 h, XRD peaks of BST, Nb_2O_5, TiO_2 and some weak $BaNb_2O_6$ phase appear [10]. It is found from Fig. 2 that the phase assembly of SBN-BST composition calcined at 800 °C is composed of BST, Nb_2O_5, new-formed $SrNb_2O_6$ and SBN. When the calcination temperature is further increased to 950 °C, XRD peaks of Nb_2O_5 and TiO_2 finally disappear, and the intensities of SBN and BST continually increase.

Figure 2 exhibits the X-ray diffraction patterns of SBN-BST powders pre-sintered at 800 °C, at different sintering temperatures for 3 h. After sintered at 820 °C for 3 h, XRD peaks of $BaNb_2O_6$ and BST phase occur.

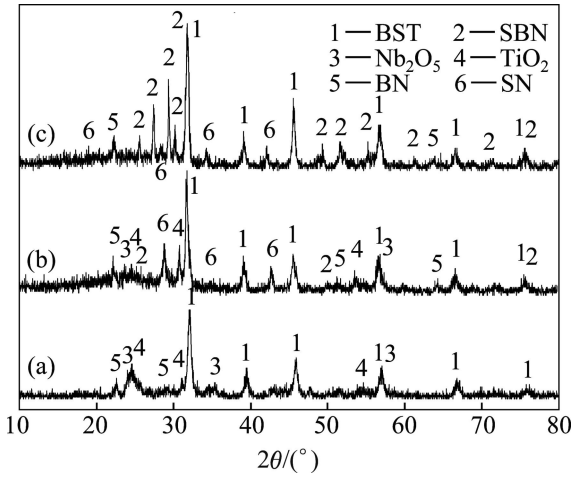

Fig. 1 XRD patterns of BSTN dry gel at different presintering temperatures for 3 h: (a) 700 °C; (b) 800 °C; (c) 950 °C

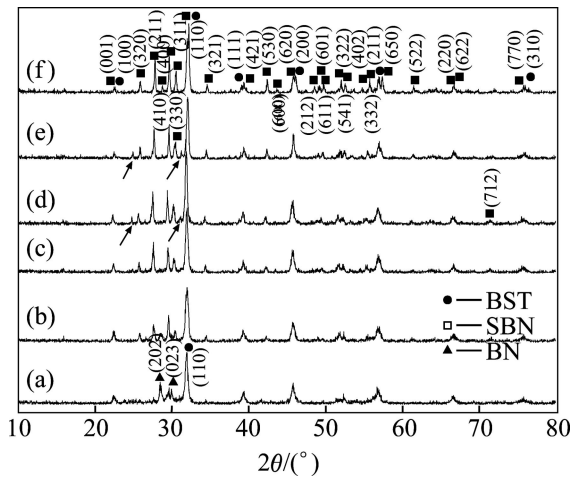

Fig.2 XRD patterns of $0.5BaO0.5Sr00.5TiO_20.5Nb_2O_5$ composite ceramics at different sintering temperatures for 3 h: (a) 820 °C; (b) 900 °C; (c) 980 °C; (d) 1050 °C; (e) 1150 °C; (f) 1200 °C

As the sintering temperature further increases to 900 °C, some weak XRD peaks of SBN appear, and XRD peaks of $BaNb_2O_6$ finally disappear. Subsequently, with the increase of sintering temperature, the diffraction peaks of SBN and BST continually increase. When the sintering temperature increases to 1150 °C, the unknown phase assigned by arrows occurs; when the sinter temperature further increases to 1200 °C, the unknown phase disappears. In Fig. 3, it can be founded clearly that

the (311) peak of SBN phase shifts to a high Bragg angle slightly while there is no change in the position of perovskite structure BST (110) peaks, which reveals that the lattice parameters of SBN phase decrease.

Figure 3 shows that the effect of Nb/Ti ratios on the valence states of Nb (3d) in the SBN-BST system. It is shown that the binding energy of Nb^{5+} $3d_{5/2}$ is 206.8 eV, and the spin-orbit splitting is 2.8 eV.

The least squares fitting method was used in above figures. The binding energy quoted for Nb^{5+} $3d_{5/2}$ in the case of CAO [11] and ATUCHIN et al [12] is in good agreement with Nb^{5+}ions in this study. From the binding

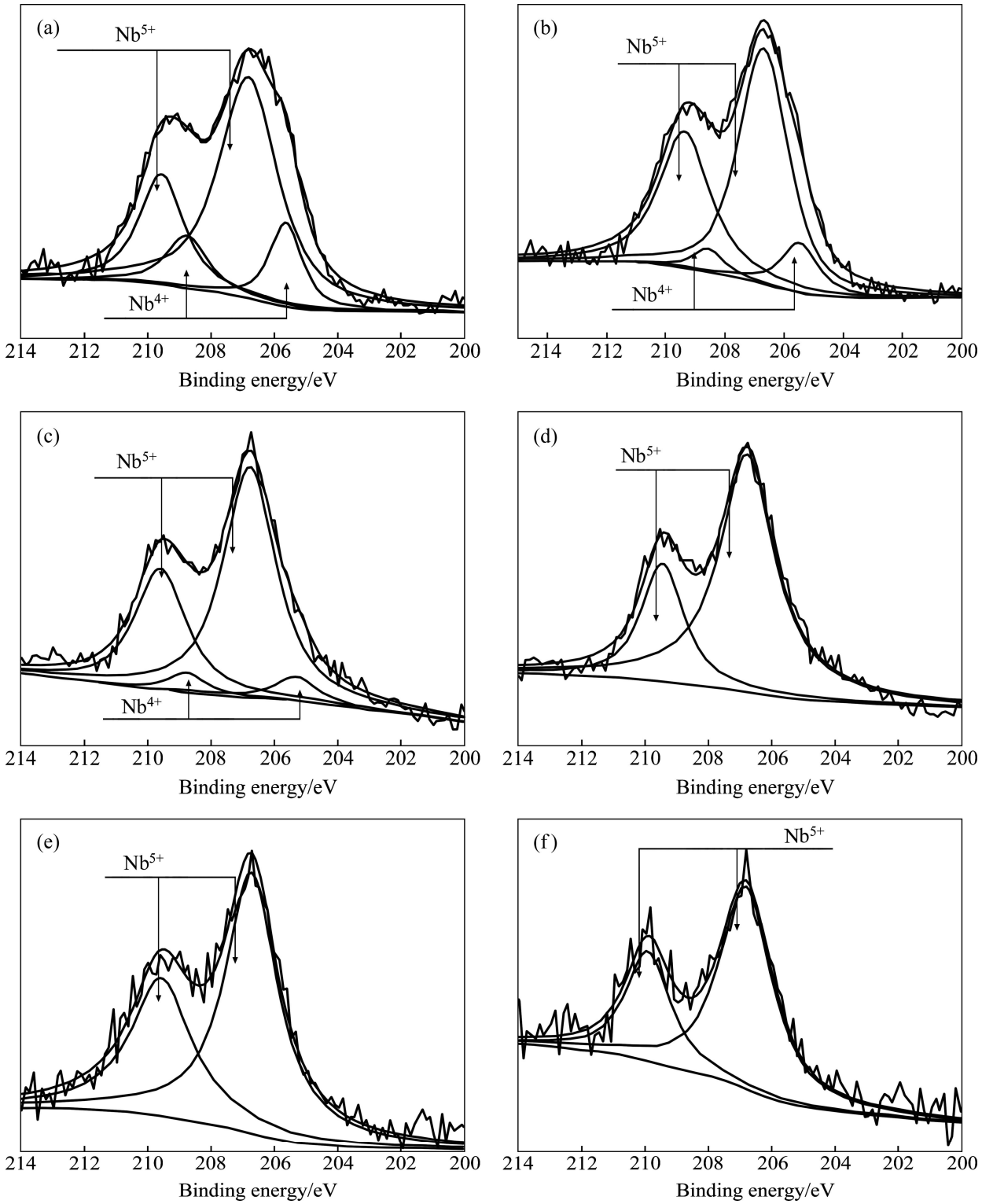

Fig. 3 XPS spectra for Nb in sintered $0.7BaO0.3SrO(1-y)TiO_2yNb_2O_5$ ceramics: (a) $y=0.1$; (b) $y=0.2$; (c) $y=0.3$; (d) $y=0.5$; (e) $y=0.6$; (f) $y=0.7$

energy, it can be concluded that the Nb^{5+} ions are present in all samples. As shown in Figs. 3 (a) and (b), the binding energy of new component is 206.1 eV, which is close to that of Nb^{4+} [13]. It is proved that there is a small part of Nb^{4+} presented in the samples (Figs. 3(a) and (b)). The mole ratio of Nb^{4+} to Nb^{5+} is 1:6.1 according to Fig. 3(a). With the increase of Nb/Ti ratios, it is found that the ratio of Nb^{4+} to Nb^{5+} ions decreases to 1: 9.4 as seen from Fig. 3 (b). Furthermore, there are no Nb^{4+} ions presented in the samples of Figs. 3(d)~(f). Therefore, the binding energies of this element strongly depend on composition. This additional pair of lines may be associated with the dissolution of Nb^{4+} ion in BST.

The high-resolution Ti spectra are present in Fig. 4 for the $0.7BaO0.3SrO0.5TiO_20.5Nb_2O_5$ composite ceramics. The detailed scans (20 eV wide) are recorded. As shown in Fig. 4 (f), Ti^{4+} ion arenot detected because of a small content. From the Figs. 4(a)−(e), only one spin-orbit doublet is observed for Ti element, the binding energy of $Ti_{2p3/2}$ is 458.3 eV, and the spin-orbit splitting is 5.8 eV. In the case of HU et al [14] and CHEN et al [15], it is concluded that the valence of Ti ion is identified as +4. Nb-doped $Ba_{0.7}Sr_{0.3}TiO_3$ is found via Ba or Sr-site vacancies, and the corresponding defect formula can be represented by

$$BaO/SrO+Nb_2O_5 \longrightarrow Ba_{Ba}/Sr_{Sr}+V''_{Ba}/V''_{Sr}+2N\dot{b}_{Ti}+6O_O \quad (1)$$

where V denotes the vacancy at the A-site.

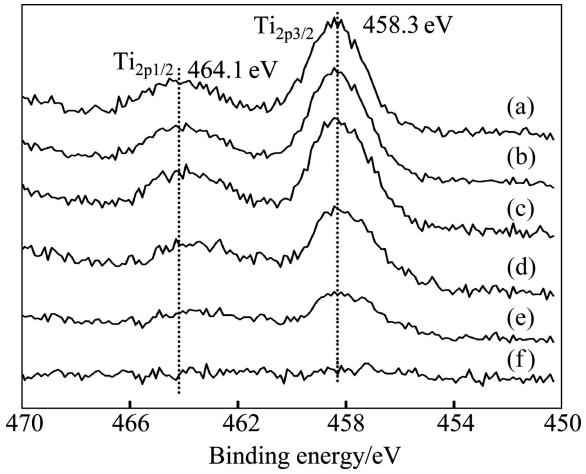

Fig. 4 XPS spectra for Ti in sintered 0.7BaO0.3SrO-(1−y) $TiO_2$$y$$Nb_2O_5$ ceramics: (a) y=0.1; (b) y=0.2; (c) y=0.3; (d) y=0.5; (e) y=0.6; (f) y=0.7

4 Conclusions

1) The beneficial effect of this powder-Sol process on preparing composite ceramics is that the process improves not only the sintering activity and densification, but also the phase uniformity and mechanical properties of the sintered body.

2) For all compositions in the Ti_{2p} spectra, only one spin-orbit doublet is observed, which indicates 4+ chemical state in the composite ceramics. The binding energies of Nb_{3d} are strongly depend on compositions.

References

[1] PATROA P K, KULKARNI A R, GUPTAB S M, HARENDRANATH C S. Improved microstructure, dielectric and ferroelectric properties of microwave-sintered $Sr_{0.5}Ba_{0.5}Nb_2O_6$ [J]. Physica B, 2007, 400: 237−242.

[2] QADRI S B, BELLOTTI J A, GARZARELLA A, WIETING T, WU D H, MAHADIK N A. Phase transition in $Sr_{0.75}Ba_{0.25}NbO_3$ near the Curie temperature [J]. Appl Phys Lett, 2006, 89: 222911-1−3.

[3] WANG X H, GU H, HUANG Q W, CEH M. Cation occupancy at the A1/A2 sites in strontium barium niobate micro-crystals grown from molten NaCl and KCl salts [J]. Acta Materialia, 2007, 55: 5304−5309.

[4] SRINIVAS A, BOEY F Y C, SRITHARAN T. Synthesis of a new electroceramic by replacement of Bi in strontium bismuth niobate [J]. J Electroceram, 2006, 16: 321−325.

[5] HUANG Q W, ZHU L H, XU J, Wang P L, Gu H, Cheng Y B. Effect of V_2O_5 on sintering behaviour, microstructure and dielectric properties of textured $Sr_{0.4}Ba_{0.6}Nb_2O_6$ ceramics [J]. J Eur Ceram Soc, 2005, 25: 957−962.

[6] JIANG S L, ZHANG.H B, LIN R Z, LIU S B, LIU M D. Electrical Properties of BST thin films fabricated by a modified sol-gel Processing [J]. Integrated Ferroelectrics, 2005, 70: 1−9.

[7] ZHOU Z H, DU P Y, WENG W J, ET AL. Dielectric properties of 0.7BaO·0.3SrO·(1−y)TiO_2·$y$$Nb_2O_5$ composite ceramics [J]. Mater Chem and Phys, 2004, 87(2/3): 430−434.

[8] NIU X K, ZHANG J L, WANG J F, LI C Y, LV Y G. Preparation and dielectric property of $Sr_xBa_{1-x}Nb_2O_6$-$Sr_{0.6}Ba_{0.4}TiO_3$ composite ceramics [J]. Electr Components and Mater, 2007, 26(4): 8−10.

[9] LIU S B, LIU M D, ZENG Y K, LIU S B, LIU M D. Preparation and characterization of $Ba_{1-x}Sr_xTiO_3$ thin films for uncooled infrared focal plane arrays [J]. Mater Sci and Eng C, 2002, 22: 73−76.

[10] SHAN L W. Preparation and pyroelectricity of strontium barium niobate/barium strontium titanate muti-phased ceramics[D]. Harbin: Harbin University of Science and Technology, 2009. (in Chinese)

[11] CAO J L, LI L T, GUI Z L. An XPS study on the degradation of lead magnesium niobate-based relax or ferroelectrics during nickel electroplating [J]. J Mater Chem, 2001, 11: 1198−1200.

[12] ATUCHIN V V, GRIVEL J C, KOROTKOV A S, ZHANG Z M. Electronic parameters of $Sr_2Nb_2O_7$ and chemical bonding [J]. J Solid State Chemistry, 2008, 181: 1285−1291.

[13] MOULDER J F, STICKLE W F, SOBOL P E, BOMBEN K D. Handbook X-ray photoelectron spectroscopy [M]. Perkin: Perkin Elmer Corporation, USA, 1992.

[14] HU Y, TAN O K, PAN J S, YAO X. A new form of nanosized $SrTiO_3$ material for near-human-body temperature oxygen sensing applications [J]. J Phys Chem B, 2004, 108: 11214−11218.

[15] CHEN J, LIAN J, WANG L M, EWING R C. X-ray photoelectron spectroscopy study of irradiation-induced amorphization of $Gd_2Ti_2O_7$ [J]. Appl Phys Lett, 2001, 79(13): 1989−1991.

粉末−凝胶法制备铌酸锶钡/钛酸锶钡陶瓷及其表征

单连伟，王凤春，王继华，吴 泽，韩志东，董丽敏，张显友

哈尔滨理工大学 材料科学与工程学院，哈尔滨 150040

摘 要：钛酸锶钡($Sr_xBa_{1-x}TiO_3$, BST)和铌酸锶钡($Sr_xBa_{1-x}Nb_2O_6$, $0.25 \leqslant x \leqslant 0.75$, SBN)是重要的铁电材料，具有优良的热电、介电和红外快速响应性能。使用廉价的 Nb_2O_5 粉末，应用粉末−溶胶工艺合成铌酸锶钡/钛酸锶钡复相陶瓷（SBN/SBT）。XRD 结果表明：钨青铜相和钙钛矿相共存于体系之中。复相陶瓷形成过程中形成了 TiO_2、$BaNb_2O_6$(BN)、$SrNb_2O_6$(SN)等中间相。干凝胶在 800 °C 下预烧 3 h，X 射线光电子能谱(XPS)分析表明，随着体系组分的变化，Ti 元素只存在＋4 价的化合态，而 Nb 元素的价态和体系的组分有关。

关键词：钛酸锶钡；铌酸锶钡；结合能

(Edited by LI Yan-hong)